# Pull-in analysis of non-uniform microcantilever beams under large deflection

Sajal Sagar Singh, Prem Pal, and Ashok Kumar Pandey'

Citation: J. Appl. Phys. **118**, 204303 (2015); doi: 10.1063/1.4936321
View online: http://dx.doi.org/10.1063/1.4936321
View Table of Contents: http://aip.scitation.org/toc/jap/118/20
Published by the American Institute of Physics

JOURNAL OF APPLIED PHYSICS **118**, 204303 (2015)

# Pull-in analysis of non-uniform microcantilever beams under large deflection

Sajal Sagar Singh,[1] Prem Pal,[2] and Ashok Kumar Pandey[1,a)]
[1]*Department of Mechanical and Aerospace Engineering, IIT Hyderabad, Kandi, Sangareddy -502285, India*
[2]*Department of Physics, IIT Hyderabad, Kandi, Sangareddy -502285 India*

(Received 17 September 2015; accepted 11 November 2015; published online 30 November 2015)

Cantilever beams under the influence of electrostatic force form an important subclass of microelectromechanical system (MEMS) and nanoelectromechanical system. Most of the studies concerning these micro-nano resonators are centered around uniform cantilever beams. In this paper, we have investigated another class of micro-resonators consisting of non-uniform cantilever beams. The study is focused around investigating pull-in voltage and resonance frequency of non-uniform cantilever beams when they operate in the linear regime about different static equilibriums. In this paper, we term this frequency as "linear frequency." Calculation of the linear frequency is done at different static equilibriums corresponding to different DC voltages. We have studied two classes of beams, one with increasing cross sectional area from the clamped edge (diverging beam) and other with decreasing cross sectional area from the clamped edge (converging beam). Within each class, we have investigated beams with linear as well as quartic variation in width. We start by obtaining Euler beam equation for non-uniform cantilever beams considering large deflection and their corresponding exact mode shapes from the linear equation. Subsequently, using the Galerkin method based on single mode approximation, we obtain static and dynamic modal equations for finding pull-in voltage and resonance frequency as a function of DC voltage, respectively. We found that the linear frequency of converging beams increases with increase in non-uniform parameter ($\alpha$) while those of diverging beams decreases with $\alpha$. A similar trend is observed for pull-in voltage. Within the converging class, beams with quartic variation in width show significant increase in both frequency and pull-in voltage as compared to corresponding linearly tapered beams. In quantitative terms, converging beams with quartic variation in width and $\alpha = -0.6$ showed an increase in linear frequency by a factor of 2.5 times and pull-in voltage by 2 times as compared to commonly used uniform beams. Our investigation can prove to be a step forward in designing highly sensitive MEMS sensors and actuators. © *2015 AIP Publishing LLC*.
[http://dx.doi.org/10.1063/1.4936321]

## I. INTRODUCTION

Electrostatically actuated microelectromechanical system (MEMS) cantilever beams form an excellent class of resonator for various devices. Most of these resonant MEMS/nanoelectromechanical system (NEMS) devices such as mass sensor, temperature sensor, and pressure sensor[1–3] operate at resonance frequency of the structure. In order to improve the performance of MEMS devices, tuning of the resonance frequency has caught attention of researchers in the past.[4–7] Attempts have been made to tune frequency of cantilever beams by reducing the dimensions to nano scale,[8] using nonlinear effect to soften or harden the system.[5–7,9] Therefore, it is vital to compute an accurate resonance frequency of such resonators during their design phase. Apart from computing resonance frequency, knowledge of the pull-in voltage is also important to achieve stable operating range.[5] A system of cantilever beam separated from the bottom electrode by a gap $d_0$ forms a parallel plate capacitance system as shown in Fig. 1(a). On application of voltage, the electrostatic force tends to attract cantilever towards fixed electrode; however, the spring force (stiffness) of cantilever resists this force. With further increase in voltage, the electrostatic force dominates, and the beam is pulled towards fixed electrode. This voltage at which restoring force could no longer balance attractive electrostatic force is known as pull-in voltage. Thus, the determination of the pull-in voltage is extremely important before designing and operating the device.

Researchers in the past have modeled resonators and obtained pull-in parameters by accounting various effects.[10–16] However, these models are limited to uniform cantilever beams. At the same time, a few studies performed the computation of frequencies of non uniform cantilever beams as well.[17–20] Mabie and Rogers[18] and Lau[19] obtained the linear frequency of double tapered beam with tip mass by expressing the mode shape in terms of Bessel functions. In yet another study, Mabie and Roger[20] analyzed the beam with constant width and linearly tapered thickness using same methodology. At the same time, special cases of tapering were also studied by William and Banerjee[21] on axially loaded beams, Auciello and Nole[22] by obtaining solution in terms of Bessel Function, and Wang[23] with the help of hypergeometric functions. For MEMS and NEMS applications, tapering in width (rather than thickness) is of interest as it is pertinent to microfabrication techniques where arbitrary planar geometry (with constant

a)Electronic mail: ashok@iith.ac.in

 

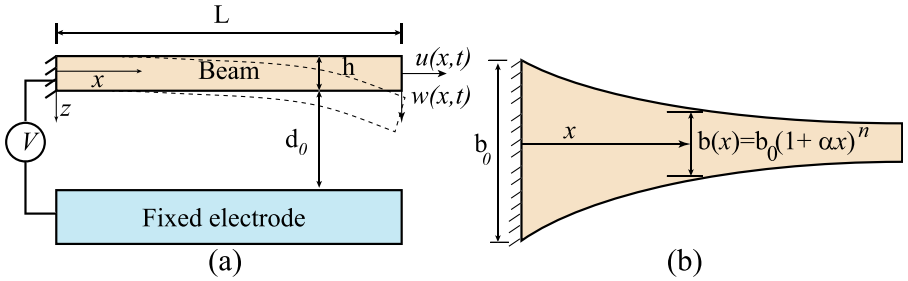


FIG. 1. (a) Transverse vibration of a cantilever beam subjected to electrostatic excitation. (b) Variation of width of a non-uniform cantilever beam with tapering parameter $\alpha$ as $b(x) = b_0(1 + \alpha x)^n$, where $n = 1$ and 4 imply beam with linear and quartic taper in width, respectively. Here, $\alpha < 0$ corresponds to converging beam, $\alpha > 0$ corresponds to diverging beams, and $\alpha = 0$ implies uniform beam. Given figure depicts a quartic converging beam with $\alpha < 0$ and $n = 4$.

thickness) can be fabricated with existing methods. In this regard, Mabie and Rogers[20] and Wang[24] numerically integrated the differential equation corresponding to the beam with varying width alone and obtained the frequency for various taper parameters. Abrate[25] proposed a method to transform the linear governing equation for special type of nonuniform width to that of a uniform beam by introducing a function. In this paper, we focus on non-uniform cantilever beam and investigate the effect of non-uniformity on frequency as well as pull-in voltage of non-uniform cantilever based resonators. In present study, we have used the transformation proposed by Abrate to find mode shape based on linear equation; however, we use this mode shape to study the influence of nonlinear curvature effect due to large DC voltage on the linear frequency of non-uniform cantilever beam using the Galerkin approach.

To compute the pull-in voltage in MEMS, several authors have worked towards obtaining its closed form expression. Nathanson *et al.*[10] obtained simplest form of pull-in voltage expression by modeling the cantilever beam as a lumped spring-mass system considering uniform gap. To include the effect of non-uniform gap between beams due to deflection with respect to fixed electrode, Pamidighantam *et al.*[11] included the effects of partial electrodes, axial stress, non-linear stiffening, charge-redistribution, fringing fields, etc., to obtain closed form expression for pull-in voltage. Osterberg and Senturia[12] proposed another closed form expression for pull-in voltage including the corrections based on finite element simulations. Chowdhury *et al.*[26] obtained a closed form model for calculating the pull in voltage based on capacitance formula given by Van Der Meijs and Fokkema.[27] Later, Ramakrishnan and Srinivasan[28] found that the model obtained by Chowdhury *et al.*[26] is limited to a range of selective dimensions. Consequently, they proposed closed form models based on different capacitance models available in literature to calculate the pull-in voltage. After validating the models with Finite Element Analysis (FEA) based software, they concluded that different capacitance models have to be used for different ranges of beam dimensions. Later, Tilmans and Legtenberg[13] used minimum energy principle to discuss pull in instability of clamped-clamped beam. To include the effect of large deformation, Chaterjee and Pohit[29] numerically studied the variation of pull-in instability for uniform cantilever beam considering the effect of large deflection. Li and Aluru[30] performed pull-in analysis in the linear, nonlinear, and mixed regime of MEMS fixed-fixed as well as cantilever beams. Based on their analysis, they concluded that different theories should be used for beams with different configurations and dimensions. A similar study was performed by Rasekh and Khadem[31] to do pull-in analysis of carbon nanotube based cantilever beams. Rahaeifard *et al.*[32] used modified coupled stress theory to capture the size effect on pull-in voltage of a nanoscaled beam. Subsequently, Baghani[33] included nonlinear geometric effects along with size effect to obtain the pull in voltage. However, most of the above studies were limited to uniform beams. To capture fringing effect due to non-uniform shape of the fixed electrode, Cheng *et al.*[34] studied pull-in parameters of rectangular cantilever torsion actuator due to electrostatic actuation with respect to elliptical, hyperbolic, and parabolic electrodes. Similarly, Lemaire *et al.*,[35] Raulli and Maute,[36] and Abdalla *et al.*[37] worked towards optimizing geometry and studied its effect on pull-in parameters. Najar *et al.*[38,39] employed differential quadrature method to study the pull-in parameters of beam with varying thickness, width, and distance from the fixed bottom electrode. Another study by Joglekar and Pawaskar[40] focused on the static pull-in analysis of linearly tapered cantilever beams using numerical technique. Almost all studies concerning non-uniform beams (fixed-fixed and cantilever) have resorted to using numerical techniques or other transformation methods to find the pull-in voltage. In this paper, we present the pull-in voltage and the frequency analysis of non-uniform cantilever beams with varying widths and nonlinear curvature effect by using the Galerkin method based on the exact mode shape of linear non-uniform cantilever beam.

To do the analysis, we first derived governing equation of motion of electrostatically excited non-uniform cantilever beam considering large deflection effect using the Hamilton's Principle based on approach described by Chaterjee and Pohit[29] for a uniform beam. Subsequently, we obtained mode shapes from linear governing equation for non-uniform cantilever beams with linear and quartic varying widths. To obtain the corresponding frequency and mode shape, we transformed linear equation for a non-uniform beam into the equations of equivalent uniform beam using method as described by Abrate.[25] However, such transformations exist for quartic tapered beam without any approximation and linearly tapered beam with some approximation. Using the appropriate boundary conditions, we finally obtained the corresponding

frequency equations and mode shapes of non-uniform beams with linear and quartic variation in width. Using mode shape of linear equation, we applied the Galerkin method based on single mode approximation to obtain nonlinear static and dynamic modal equations. Subsequently, we obtained the pull-in voltage as well as frequency of non-uniform beam with different types of tapering. After validating the model with available results, we discuss the effects of tapering on pull-in voltage as well as linear frequency of non-uniform beams.

## II. EQUATION OF MOTION

In this section, we derive governing equation of transverse motion $w(x,t)$ along $z$ direction considering large deflection for nonuniform cantilever beam under the influence of electrostatic force $Q_s$ as shown in Fig. 1. To derive the equation, we consider a cantilever beam of length $L$, width $b(x)$, thickness $h$, area moment of inertia $I(x)$, density $\rho$, and effective modulus $E = \frac{E'}{(1-v^2)}$, where $E'$ is the Young's modulus, and $v$ is the Poisson's ratio. If $u(x, t)$ is an axial extension under large deflection, then the axial strain $\zeta_{xx}$ at neutral axis can be written as[41]

$$\zeta_{xx} = \sqrt{\left(1+\frac{\partial u(x,t)}{dx}\right)^2 + \left(\frac{\partial w(x,t)}{dx}\right)^2} - 1, \tag{1}$$

and the curvature $k$ as[42]

$$k = \left(1+\frac{\partial u}{\partial x}\right)\frac{\partial^2 w}{\partial x^2} - \frac{\partial^2 u}{\partial x^2}\frac{\partial w}{\partial x}. \tag{2}$$

Writing the kinetic energy $KE$ and bending strain energy $U_s$ as

$$KE = \frac{1}{2}\int_0^{\mathbf{L}} \rho A(x)\{\dot{u}^2 + \dot{w}^2\}dx,$$
$$U_s = \frac{1}{2}\int_0^{\mathbf{L}} EI(x)k^2 dx,$$

and then using the virtual work done by external force such that $\delta Q = Q_s$, we apply the Hamilton's principle

$$\int_{t_1}^{t_2} (\delta KE - \delta U_s - \delta Q)dt = 0, \tag{3}$$

to obtain the governing equation. After substituting the energy expression and using an approximate expression of $u' = -w'^2/2$ under inextensibility condition, i.e., $\zeta_{xx} = 0$, the governing equation with non-linear terms upto $O(\epsilon^3)$ for undamped forced vibration can be written as

$$\rho A(x)\ddot{w} - EI(x)(w'')^3 + w'\rho A(x) \times \int_0^x (w'\ddot{w}' + (\dot{w}')^2)dx + w'(EI(x)w''w')'' + (EI(x)w'')'' = Q_s(t), \tag{4}$$

where $Q_s(t)$ is the electrostatic force considering fringing field effect which is given by[40]

$$Q_s(t) = \frac{1}{2}\frac{\epsilon_0 b(x)(V+v(t))^2}{(d_0-w)^2}\left(1+\frac{2(d_0-w)}{\pi b(x)}\right), \tag{5}$$

where $\epsilon_0 = 8.854 \times 10^{-12}$ F/m is the permittivity of free space, $V$ is DC voltage, and $v(t)$ is AC voltage.

The boundary conditions for non-uniform cantilever beam can be written as

$$w(0) = \left.\frac{\partial w}{\partial x}\right|_{x=0} = 0, \quad \left.\frac{\partial^2 w}{\partial x^2}\right|_{\mathbf{x=L}} = 0,$$
$$\left.\frac{\partial}{\partial x}\left(EI(x)\frac{\partial^2 w}{\partial x^2}\right)\right|_{\mathbf{x=L}} = 0. \tag{6}$$

### A. Non-dimensionalisation

To obtain non-dimensional form of governing equation given by Eq. (4) and boundary conditions given by Eq. (6), we define the following non-dimensional parameters:

$$x^* = \frac{x}{L}, \quad w^* = \frac{w}{d_0}, \quad t^* = \frac{t}{\left(L^2\sqrt{\frac{\rho A_0}{EI_0}}\right)}, \quad \gamma = \frac{d_0}{\mathrm{L}},$$
$$f_1(x) = \frac{E\tilde{I}(x)}{EI_0}, \quad f_2(x) = \frac{\rho\tilde{A}(x)}{\rho A_0}, \tag{7}$$

where $EI(x) = EI_0 + E\tilde{I}(x) = (1+f_1(x))EI_0$ and $\rho A(x) = \rho A_0 + \rho\tilde{A}(x) = (1+f_2(x))\rho A_0$, $I_0$ and $A_0$ are the area moment of inertia and cross-sectional area at the fixed end of cantilever beam, respectively. We substitute nondimensional parameters in Eqs. (4) and (6) rearrange the terms to get the equivalent non-dimensional governing equation as (after dropping the superscript * for convenience)

$$(1+f_2(x))\ddot{w} + \left((1+f_1(x))w''\right)'' - \gamma^2(1+f_1(x)) \times (w'')^3 + \gamma^2(1+f_3(x))w'\int_0^x \left((\dot{w}')^2 + w'\ddot{w}'\right)dx + \gamma^2 w' \times \left((1+f_1(x))w''w'\right)'' - \frac{1}{2}\frac{\epsilon_0 b(x)(V+v(t))^2 L}{\gamma^3 EI_0(1-w)^2} - \frac{\epsilon_0(V+v(t))^2L^2}{\pi\gamma^2 EI_0(1-w)} = 0, \tag{8}$$

and the boundary condition as

$$w(0) = \left.\frac{\partial w}{\partial x}\right|_{x=0} = 0, \left.\frac{\partial^2 w}{\partial x^2}\right|_{x=1} = 0,$$
$$\left.\frac{\partial}{\partial x}(1+f_1(x))\frac{\partial^2 w}{\partial x^2}\right|_{x=1} = 0. \tag{9}$$

In Sec. II B, we obtain exact mode shape from linear undamped equation under free vibration corresponding to uniform as well as non-uniform beams.

### B. Derivation of linear mode shape

In this section, we obtain exact mode shape of cantilever beam with uniform as well as linear and quartic tapering in width. To obtain the mode shape, we consider governing

equation under linear, undamped, and free vibration conditions, thus, neglecting the nonlinear, damping, and forcing terms. After substituting the expressions for $f_1$ and $f_2$ in Eq. (8), the resulting linear equation for non-uniform beam can be written as

$$\frac{\partial^2}{\partial x^2}\left((EI(x))\frac{\partial^2 w}{\partial x^2}\right)+\frac{EI_0}{\rho A_0}(\rho A(x))\frac{\partial^2 w}{\partial t^2}=0. \tag{10}$$

To obtain mode shape, we convert the equation for non-uniform beam into an equivalent governing equation of uniform beam by following the approach as proposed by Abrate.[26] Taking a function $\sigma(x)$ such that $v(x)=\sigma(x)w(x)$, the equation for uniform beam can be written as

$$\frac{\partial^4(\sigma w)}{\partial x^4}+\frac{\partial^2(\sigma w)}{\partial t^2}=0. \tag{11}$$

Writing the expanded form of Eqs. (10) and (11) as

$$(I''w''+Iw''''+2I'w''')+\frac{I_0}{A_0}A(x)\ddot{w}=0, \tag{12}$$

and

$$(\sigma''''w+4\sigma'''w'+6\sigma''w''+4\sigma'w'''+\sigma w'''')+\sigma\ddot{w}=0, \tag{13}$$

and then comparing the terms on left hand side of Eqs. (12) and (13), we get the following relationship:

$$\frac{6\sigma''}{I''}=\frac{4\sigma'}{2I'}=\frac{\sigma}{I}=\frac{A_0\sigma}{I_0A(x)}. \tag{14}$$

Taking $\sigma(x)$ such that $\sigma''''$ and $\sigma'''$ are either zero or negligible, and satisfying Eq. (14), we find $\sigma(x)$, $I(x)$ and $A(x)$ corresponding to each type of tapered beam, separately. Consequently, for computed form of $\sigma$, $I(x)$, and $A(x)$, Eq. (10) for non-uniform beam and Eq. (11) for uniform beam with $v(x)=\sigma w$ become equivalent. Based on equivalent uniform beam, the exact mode shape for Eq. (11) is readily available as[43]

$$v(x)=A_1\sin(\lambda x)+A_2\cos(\lambda x)+A_3e^{\lambda x}+A_4e^{-\lambda x}. \tag{15}$$

Using boundary conditions for cantilever beam, the form of mode shape can be rewritten as

$$v(x)=\sigma(x)w(x)=A_1\left[\sin(\lambda x)-\sinh(\lambda x)-\frac{\sin(\lambda x)+\sinh(\lambda x)}{\cos(\lambda x)+\cosh(\lambda x)}(\cos(\lambda x)+\cosh(\lambda x))\right]. \tag{16}$$

Finally, the mode shape of non-uniform beam with given tapering can be found from the relation $w(x)=\frac{v(x)}{\sigma(x)}$. Now, we apply above concept in computing mode shapes of uniform and non-uniform beams with different types of tapering and mention the frequency equation to obtain corresponding frequency parameter, $\lambda$.

1. Uniform beam: For uniform cantilever beam, we get $\sigma(x)=1$, $A(x)=A_0$, and $I(x)=I_0$. Consequently, for $v(x)=w(x)$, the mode shape is given by Eq. (16). Using appropriate boundary conditions, the value of frequency parameter $\lambda$ can be numerically obtained by solving the following transcedental equation:

$$2\lambda^6(2+e^{\lambda}\cos(\lambda)+e^{-\lambda}\cos(\lambda))=0. \tag{17}$$

2. Non-uniform beam with linear tapering: For a non-uniform cantilever beam with linearly tapered width, $b(x)=b_0(1+\alpha x)$, where $-1<\alpha<0$ corresponds to converging type and $\alpha>0$ corresponds to diverging case. The area moment of inertia and area can be written as $I(x)=I_0(1+\alpha x)$ and $A(x)=A_0(1+\alpha x)$, respectively. The corresponding expression of $\sigma$ can be obtained from Eq. (14) as $\sigma(x)=\sqrt{(1+\alpha x)}$, thus, $A(x)=A_0\sigma(x)^2$ and $I(x)=I_0\sigma(x)^2$. Since the above relationship of $\sigma$ and $\alpha$ in case of linearly tapered width is obtained by neglecting higher order differential terms $\sigma''''$ and $\sigma'''$, the error associated with such assumptions grows rapidly as $|\alpha|>0.5$. For given boundary condition, the frequency parameter $\lambda$ can be found from the frequency equation

$$\begin{aligned}&\frac{\lambda^2}{8(1+\alpha)^4}\big(16\cos(\lambda)e^{\lambda}\alpha^4\lambda^4+64\cos(\lambda)e^{-\lambda}\\&\times\alpha\lambda^4+12\cos(\lambda)e^{-\lambda}\alpha^4\lambda+64\cos(\lambda)e^{\lambda}\alpha\lambda^4\\&-12\cos(\lambda)e^{\lambda}\alpha^4\lambda-48\sin(\lambda)e^{-\lambda}\alpha^2\lambda^3\\&+12\sin(\lambda)e^{-\lambda}\alpha^4\lambda+64\cos(\lambda)e^{-\lambda}\alpha^3\lambda^4\\&+96\cos(\lambda)e^{\lambda}\alpha^2\lambda^4+16\cos(\lambda)e^{-\lambda}\alpha^4\lambda^4+32\lambda^4\\&-6\alpha^4+192\alpha^2\lambda^4+32\alpha^4\lambda^4+128\alpha^3\lambda^4\\&+128\alpha\lambda^4+64\cos(\lambda)e^{\lambda}\alpha^3\lambda^4+48\cos(\lambda)e^{-\lambda}\alpha^2\\&\times\lambda^3+16\cos(\lambda)e^{-\lambda}\alpha^4\lambda^3+48\alpha^3\lambda^3e^{-\lambda}\cos(\lambda)\\&-48\cos(\lambda)e^{\lambda}\alpha^2\lambda^3-16\cos(\lambda)e^{\lambda}\alpha^4\lambda^3-48\\&\times\cos(\lambda)e^{\lambda}\alpha^3\lambda^3+12e^{\lambda}\sin(\lambda)\alpha^3\lambda+16e^{-\lambda}\alpha\lambda^3\\&\times\cos(\lambda)+12e^{-\lambda}\sin(\lambda)\alpha^3\lambda-16e^{\lambda}\cos(\lambda)\alpha\lambda^3\\&+96\cos(\lambda)e^{-\lambda}\alpha^2\lambda^4-12e^{\lambda}\cos(\lambda)\alpha^3\lambda-16e^{\lambda}\alpha\lambda^3\\&\times\sin(\lambda)+12\cos(\lambda)e^{-\lambda}\alpha^3\lambda-16e^{-\lambda}\sin(\lambda)\alpha\lambda^3\\&+16e^{\lambda}\lambda^4\cos(\lambda)+3e^{\lambda}\alpha^4\cos(\lambda)+e^{-\lambda}16\cos(\lambda)\lambda^4\\&+3e^{-\lambda}\alpha^4\cos(\lambda)-48\sin(\lambda)e^{\lambda}\alpha^2\lambda^3+12\sin(\lambda)\\&\times e^{\lambda}\alpha^4\lambda-48\sin(\lambda)e^{\lambda}\alpha^3\lambda^3-48\sin(\lambda)\lambda^3e^{-\lambda}\alpha^3\\&-16e^{\lambda}\sin(\lambda)\alpha^4\lambda^3-16\sin(\lambda)e^{-\lambda}\alpha^4\lambda^3)=0.\end{aligned} \tag{18}$$

Finally, for given $\lambda$ and $\sigma$, the mode shape can be obtained from $w(x)=\frac{v(x)}{\sigma(x)}$, where $v(x)$ is given by Eq. (16).

3. Non-uniform beam with quartic tapering: For a non-uniform cantilever beam with quartic variation in width, we take $b(x)=b_0(1+\alpha x)^4$, where $-1<\alpha<0$ corresponds to converging type and $\alpha>0$ corresponds to diverging case. Although there is no restriction over validity of Eq. (14) in this case, we restrict the value of $\alpha$ to 0.6 for quartic tapered beam. The area moment of inertia and area can be written as $I(x)=I_0(1+\alpha x)^4$ and $A(x)=A_0(1+\alpha x)^4$, respectively. Corresponding expression of $\sigma$ can be obtained from Eq. (14) as $\sigma(x)=(1+\alpha x)^2$, thus, $A(x)=A_0\sigma(x)^2$ and $I(x)=I_0\sigma(x)^2$. The frequency parameter $\lambda$ can be found from the frequency equation

$$\frac{2\lambda^2}{(1+\alpha)^4}\left(-12\sin(\lambda)e^{-\lambda}\alpha^4\lambda - 4e^{\lambda}\cos(\lambda)\times\alpha\lambda^3 - 12e^{\lambda}\sin(\lambda)\alpha^3\lambda + 4e^{-\lambda}\cos(\lambda)\alpha\lambda^3 + 24e^{\lambda}\sin(\lambda)\alpha^3\lambda^2 - 12e^{\lambda}\sin(\lambda)\alpha^2\lambda^3 - 24\right.$$
$$\times e^{-\lambda}\sin(\lambda)\alpha^3\lambda^2 - 12e^{-\lambda}\sin(\lambda)\alpha^2\lambda^3 + 12e^{\lambda}\times\cos(\lambda)\alpha^4\lambda - 12e^{\lambda}\cos(\lambda)\alpha^2\lambda^3 + 4e^{\lambda}\cos(\lambda)$$
$$\times\alpha\lambda^4 - 12e^{-\lambda}\cos(\lambda)\alpha^4\lambda + 12e^{-\lambda}\cos(\lambda)\times\alpha^2\lambda^3 + 4e^{-\lambda}\cos(\lambda)\alpha\lambda^4 + e^{\lambda}\cos(\lambda)\alpha^4\lambda^4$$
$$+e^{-\lambda}\cos(\lambda)\alpha^4\lambda^4 - 4e^{\lambda}\sin(\lambda)\alpha^4\lambda^3 - 4e^{-\lambda}\alpha^4\times\sin(\lambda)\lambda^3 - 4e^{\lambda}\cos(\lambda)\alpha^4\lambda^3 + 4e^{\lambda}\cos(\lambda)\alpha^3\lambda^4$$
$$+4e^{-\lambda}\cos(\lambda)\alpha^4\lambda^3 + 4e^{-\lambda}\cos(\lambda)\alpha^3\lambda^4 + 12e^{\lambda}\times\sin(\lambda)\alpha^4\lambda^2 - 12e^{\lambda}\sin(\lambda)\alpha^3\lambda^3 - 12e^{-\lambda}\sin(\lambda)$$
$$\times\alpha^4\lambda^2 - 12e^{-\lambda}\sin(\lambda)\alpha^3\lambda^3 - 12e^{\lambda}\cos(\lambda)\times\alpha^3\lambda^3 + 6e^{\lambda}\cos(\lambda)\alpha^2\lambda^4 + 12e^{-\lambda}\cos(\lambda)$$
$$\times\alpha^3\lambda^3 + 6e^{-\lambda}\cos(\lambda)\alpha^2\lambda^4 - 12e^{\lambda}\sin(\lambda)\alpha^4\lambda + 12e^{\lambda}\cos(\lambda)\alpha^3\lambda + 12e^{\lambda}\sin(\lambda)\alpha^2\lambda^2 - 4e^{\lambda}$$
$$\times\sin(\lambda)\alpha\lambda^3 - 12e^{-\lambda}\cos(\lambda)\alpha^3\lambda - 12e^{-\lambda}\times\sin(\lambda)\alpha^2\lambda^2 - 4e^{-\lambda}\sin(\lambda)\alpha\lambda^3 + 24\alpha^4 - 12\alpha^3$$
$$\times e^{-\lambda}\sin(\lambda)\lambda - 12e^{-\lambda}\cos(\lambda)\alpha^4 + e^{\lambda}\cos(\lambda)\lambda^4$$
$$\left.+e^{-\lambda}\cos(\lambda)\lambda^4 - 12e^{\lambda}\cos(\lambda)\alpha^4 + 8\alpha\lambda^4 + 2\alpha^4\lambda^4 + 8\alpha^3\lambda^4 + 12\alpha^2\lambda^4 + 2\lambda^4\right) = 0. \tag{19}$$

Like linearly tapered beam, for given $\lambda$ and $\sigma$, the mode shape can be obtained from $w(x) = \frac{v(x)}{\sigma(x)}$, where $v(x)$ is given by Eq. (16).

### C. Static and dynamic equations

To determine pull-in voltage and frequency at different DC voltages, we first obtain the static and dynamic deflection equations for non-uniform cantilever beams with different tapers. Since the net transverse deflection, $w(x, t)$, is composed of a static deflection $z_s(x)$ due to application of DC bias and dynamic deflection $z(x, t)$ due to AC voltage, $w(x, t)$ becomes

$$w(x,t) = z_s(x) + z(x,t). \tag{20}$$

Substituting the assumed deflection in nondimensional governing equation as given by Eq. (8) and setting the time-varying dynamic terms as zero, we obtain equation governing static deflection as

$$f_1''z_s'' + 2f_1'z_s''' + (1+f_1)z_s'''' - \gamma^2(1+f_1)(z_s'')^3$$
$$+\gamma^2 z_s'\left(f_1''z_s''z_s' + 2f_1'z_s'''z_s' + 2f_1'(z_s'')^2 + (1+f_1)z_s''''z_s'\right.$$
$$\left.+ 3(1+f_1)z_s'''z_s''\right) - \frac{1}{2}\frac{\epsilon_0 b(x)V^2L}{\gamma^3 EI_0(1-z_s)^2} - \frac{\epsilon_0 V^2L^2}{\pi\gamma^2 EI_0(1-z_s)} = 0. \tag{21}$$

Similarly, the dynamic equation is obtained by substituting Eq. (20) in Eq. (8), where the static deflection $z_s$ is obtained from Eq. (21). Expanding the forcing term about $z = 0$ and retaining terms upto first order, we obtain corresponding linear dynamic equation by neglecting the nonlinear terms and forcing terms as

$$(1+f_2)\ddot{z} + (1+f_1)z'''' + \left(4z_s'z''f_1'\gamma^2 + 3\gamma^2 z_s'f_1z''' + 2\gamma^2 z_s'f_1''z' + 3\gamma^2 z_s'f_1z''' + 3\gamma^2 z_s'z''' + 3\gamma^2 z_s'z'''\right)z_s''$$
$$+\left(\left(-3\gamma^2f_1 - 3\gamma^2\right)(z_s'')^2 + \gamma^2(z_s')^2f_1'' + 3\gamma^2z_s'f_1z''' + 3\gamma^2z_s'z''' + f_1''\right)z'' + \left(2\gamma^2z_s'f_1z'''' + 4\gamma^2z_s'f_1'z''' + 2\gamma^2f_1'(z_s'')^2 + 2\gamma^2z_s'z''''\right)z'$$
$$+\left(\gamma^2f_1z'''' + 2\gamma^2f_1'z''' + \gamma^2z''''\right)(z_s')^2 + \left(\gamma^2\int_0^x\left(z'''z_s'f_2 + z'''z_s'\right)dx\right)z_s' + 2f_1'z''' - \frac{\epsilon_0V^2L}{\gamma^2EI_0}\left(\frac{b(x)}{\gamma(1-z_s)^3} + \frac{L}{\pi(1-z_s)^2}\right)z = 0. \tag{22}$$

## III. REDUCED ORDER MODEL

In order to find the reduced order equations, we approximate static and dynamic deflections based on first transverse mode as $z(x,t) = P(t)\phi(x)$ and $z_s = A\phi(x)$, respectively, where $\phi(x)$ is the mode shape of non-uniform cantilever beam with different tapering as obtained in Section III. However, it is to be noted that for the first flexural mode, the static deflection due to applied DC is not very different from the mode shape. As a result, the static deflection is assumed in terms of the mode shape. However, this approximation is valid only for the first resonance mode. At higher modes, the shape of static deflection will no longer be equal to dynamic deflection, i.e., the mode shape. Here, we carried out further analysis only for the first resonance mode. Subsequently, we apply the Galerkin method to reduce static and dynamic equations given by Eqs. (21) and (22), respectively, to reduced order form. The reduced form of static equation governing amplitude of static deflection $A$ is given by

$$\left(\int_0^1 (f_1''\phi(x)''\phi(x) + 2f_1'\phi(x)'''\phi(x) + (1+f_1)\phi(x)\phi(x)'''')dx\right)A + \left(\int_0^1 \left(-\gamma^2(1+f_1)\times(\phi(x)'')^3\phi(x) + \gamma^2(\phi(x)')^2 f_1''\phi(x)''\phi(x) + \gamma^2\phi(x)'2f_1'\phi(x)'''\phi(x)'\phi(x) + 2\gamma^2 f_1'(\phi(x)'')^2 \times\phi(x)\phi(x)' + (1+f_1)\gamma^2(\phi(x)')^2\phi(x)''''\phi(x) + 3(1+f_1)\gamma^2\phi(x)'\phi(x)\phi(x)'''\phi(x)''\right)dx\right)A^3 - \frac{1}{2}\frac{\epsilon_0 V^2 L}{\gamma^3 EI_0}\int_0^1\left(\frac{b(x)\phi(x)}{(1-A\phi(x))^2}\right)dx - \frac{\epsilon_0 V^2 L^2}{\pi\gamma^2 EI_0}\times\int_0^1\left(\frac{\phi(x)}{(1-A\phi(x))}\right)dx = 0, \tag{23}$$

and the dynamic equation becomes

$$\left[\int_0^1 (1+f_2)(\phi(x))^2 dx\right]\ddot{P} + \left[\int_0^1 [(1+f_1)\times\phi(x)'''' + \left((4\phi(x)'\phi(x)''f_1'\gamma^2 + 3\gamma^2\phi(x)'\times f_1\phi(x)''' + 2\gamma^2\phi(x)'f_1''\phi(x)' + 3\gamma^2\phi(x)' \times f_1\phi(x)''' + 3\gamma^2\phi(x)'\phi(x)''' + 3\gamma^2\phi(x)'\times\phi(x)''')\phi(x)'' + \left(\left(-3\gamma^2 f_1 - 3\gamma^2\right)(\phi(x)'')^2 + \gamma^2(\phi(x)')^2 f_1'' + 3\gamma^2\phi(x)'f_1\phi(x)''' + 3\gamma^2\phi(x)'\times\phi(x)''' + f_1''\right)\phi(x)'' + \left(\gamma^2\int_0^x \phi(x)'''\phi(x)'f_2 + \phi(x)'''\phi(x)'\right)dx\right)\phi(x)' + \left(\left(2\gamma^2\phi(x)'f_1\phi(x)'''' + 4\gamma^2\phi(x)'f_1'\phi(x)''' + 2\gamma^2 f_1'(\phi(x)'')^2 + 2\gamma^2\times\phi(x)'\phi(x)''''\right)\phi(x)' + \left(\gamma^2 f_1\phi(x)'''' + 2\gamma^2 f_1'\times\phi(x)''' + \gamma^2\phi(x)''''\right)(\phi(x)')^2\right))A^2 + 2f_1'\phi(x)''' - \frac{\epsilon_0 V^2 L}{\gamma^2 EI_0}\left(\frac{b(x)\phi(x)}{\gamma(1-A\phi(x))^3} + \frac{L}{\pi}\frac{\phi(x)}{(1-A\phi(x))^2}\right)\right]\phi(x)dx\Bigg]P = 0. \tag{24}$$

In Secs. III A and III B, we obtain pull-in voltage and frequency variation of first transverse mode of non-uniform beams.

### A. Pull-in voltage

Pull-in voltage is the DC voltage at which the electrostatic force becomes equal to elastic force. Consequently, the static deflection of beam approaches to infinite when the voltage increases beyond pull-in voltage, i.e., $\frac{dA}{dV}|_{V=V_{PI}} \to \infty$ or $\frac{dV}{dA}|_{V=V_{PI}} = 0$. Therefore, in order to obtain pull-in voltage, we differentiate the reduced form of static equation given by Eq. (23) with respect to A to get

$$\left(\int_0^1 (f_1''\phi(x)''\phi(x) + 2f_1'\phi(x)'''\phi(x) + (1+f_1)\times\phi(x))\phi(x)''''dx\right) + 3\left(\int_0^1 \left(-\gamma^2(1+f_1)\phi(x)\times(\phi(x)'')^3 + \gamma^2(\phi(x)')^2 f_1''\phi(x)''\phi(x) + \gamma^2\times\phi(x)'2f_1'\phi(x)'''\phi(x)'\phi(x) + 2\gamma^2\phi(x)'f_1' \times(\phi(x)'')^2\phi(x) + (1+f_1)\gamma^2(\phi(x)')^2\phi(x)\times\phi(x)'''' + 3(1+f_1)\gamma^2\phi(x)\phi(x)'\phi(x)''\phi(x)''')\times dx\right)A^2 - \frac{\epsilon_0 L}{\gamma^2 EI_0}\left[\frac{V}{\gamma}\frac{dV}{dA}\int_0^1\left(\frac{b(x)\phi(x)}{(1-A\phi(x))^2}\right)dx + \frac{V^2}{\gamma}\int_0^1\left(\frac{b(x)\phi(x)^2}{(1-A\phi(x))^3}\right)dx + \frac{2LV}{\pi}\frac{dV}{dA}\int_0^1\left(\frac{\phi(x)}{(1-A\phi(x))}\right)dx + \frac{LV^2}{\pi}\times\int_0^1\left(\frac{\phi(x)^2}{(1-A\phi(x))^2}\right)dx\right] = 0. \tag{25}$$

After substituting $\frac{dV}{dA}|_{V=V_{PI}} = 0$ for the condition at pull-in, we obtain the following expression of pull-in voltage:

$$V_{PI} = \left[\frac{\gamma^2 EI_0}{\epsilon_0 L}\frac{S}{E}\right]^{\frac{1}{2}}, \tag{26}$$

where

$$E = \left[\frac{1}{\gamma}\int_0^1\left(\frac{b(x)\phi(x)^2}{(1-A_{PI}\phi(x))^3}\right)dx + \frac{L}{\pi}\int_0^1\left(\frac{\phi(x)^2}{(1-A_{PI}\phi(x))^2}\right)dx\right],$$

and

$$S = \int_0^1 [f_1''\phi(x)''\phi(x) + 2f_1'\phi(x)'''\phi(x) + (1+f_1)\phi(x)\phi(x)'''']dx + 3A_{PI}^2 \times \int_0^1 [-\gamma^2(1+f_1)(\phi(x)'')^3\phi(x) + \gamma^2(\phi(x)')^2 f_1''\phi(x)''\phi(x) + \gamma^2\phi(x)'2f_1'\phi(x)''' \times \phi(x)'\phi(x) + 2\gamma^2\phi(x)'f_1'(\phi(x)'')^2\phi(x) + (1+f_1)\gamma^2(\phi(x)')^2\phi(x)''''\phi(x) + 3(1+f_1) \times \gamma^2\phi(x)'\phi(x)\phi(x)'''\phi(x)'']dx,$$

where $A_{PI}$ is the static deflection at pull-in voltage. The static deflection from Eq. (23) at pull-in parameters is solved along with Eq. (26) to obtain the pull-in voltage.

### B. Normal mode frequency

To find the frequency of first transverse mode of the system, we re-write Eq. (24) of dynamic deflection in the following form:

$$M\ddot{P} + KP = 0. \tag{27}$$

Consequently, the frequency $\omega$ of oscillating cantilever beam about statically deflected position due to applied DC is given by

$$\omega = \sqrt{\frac{K}{M}}. \tag{28}$$

On comparing Eqs. (24) and (27), we get the expression for $M$ and $K$ in terms of amplitude of static deflection $A$, DC Voltage $V$, beam dimensions, and properties as

$$M = \int_0^1 (1+f_2)(\phi(x))^2 dx,$$

and

$$K = \int_0^1 \Big[(1+f_1)\phi(x)'''' + \Big(\big(4\phi(x)'\phi(x)''f_1'\gamma^2 + 3\gamma^2\phi(x)'f_1\phi(x)''' + 2\gamma^2\phi(x)'f_1''\phi(x)' + 3\gamma^2\phi(x)' \times f_1\phi(x)''' + 3\gamma^2\phi(x)'\phi(x)''' + 3\gamma^2\phi(x)'\phi(x)''')\phi(x)'' + \Big(\big(-3\gamma^2 f_1 - 3\gamma^2\big)\big(\phi(x)''\big)^2 + \gamma^2\big(\phi(x)'\big)^2 f_1'' + 3\gamma^2 \times \phi(x)'f_1\phi(x)''' + 3\gamma^2\phi(x)'\phi(x)''' + f_1'')\phi(x)'' + \Big(\gamma^2\int_0^x \phi(x)'''\phi(x)'f_2 + \phi(x)'''\phi(x)'\Big)dx)\phi(x)' + \Big(\big(2\gamma^2\phi(x)'f_1\phi(x)'''' + 4\gamma^2\phi(x)'f_1'\phi(x)''' + 2\gamma^2 f_1' \times \big(\phi(x)''\big)^2 + 2\gamma^2\phi(x)'\phi(x)''''\big)\phi(x)' + \big(\gamma^2 f_1\phi(x)'''' + 2\gamma^2 f_1'\phi(x)''' + \gamma^2\phi(x)''''\big)\big(\phi(x)'\big)^2\Big)\Big)A^2 + 2f_1'\phi(x)''' - \frac{\epsilon_0 V^2 L}{\gamma^2 E I_0}\left(\frac{b(x)\phi(x)}{\gamma(1-A\phi(x))^3} + \frac{L}{\pi}\frac{\phi(x)}{(1-A\phi(x))^2}\right)\Big]\phi(x)dx.$$

Finally, it is important to note that the frequency equation considers nonlinear curvature effect which becomes important at large static deflection under large DC voltage. Any nonlinearity in the motion amplitude of AC component, leading to so-called Duffing resonance, is not considered in this paper.

## IV. RESULTS AND DISCUSSION

In this section, we discuss the effect of non-uniformity parameter, $\alpha$, on above mentioned phenomenon for the uniform beam as well as beams with linear and quartic taper in width. Again, we mention that $\alpha > 0$ and $-1 < \alpha < 0$ correspond to diverging and converging beams, respectively. The uniform beam corresponds to the case when $\alpha = 0$. In Sec. IV A, we discuss the effect of taper parameter on linear frequency at zero DC voltage, when nonlinear curvature effect is negligible for different beams. Subsequently, we use the linear mode of different tapered beams to obtain pull-in voltage and frequency of non-uniform cantilever beam with nonlinear curvature effects. Finally, we compare results with available values in literature for some cases and then discuss about the importance of tapering.

### A. Frequency analysis at zero DC voltage

The transcendental Eqs. (17), (18), and (19) corresponding to the uniform beam, beams with linear tapers, and beams with quartic tapers, respectively, can be solved numerically to obtain resonance frequencies for different $\alpha$. Although, these equations can be used to obtain frequencies for higher modes as well, here, we compute the frequency of only first flexural mode. Frequencies for all the three cases for various $\alpha$ are tabulated in Tables I and II, where $\alpha = 0$ corresponds to uniform beam. Results for uniform and linearly converging beams are also compared with that of Mabie and Roger[20] in which the linear frequency is obtained using numerical integration without finding the mode shape. As previously mentioned in Section II B, the transformation of linearly tapered beam into equivalent uniform beam is done with some approximation. The effect of this approximation can be observed from Table I. By comparing the

TABLE I. The non dimensional fundamental frequency of converging (negative α) and diverging (positive α) beam with linear taper in width.

| α | Present | Mabie and Roger[20] |
|---|---|---|
| 0.0 | 3.516 | 3.516 |
| −0.1 | 3.628 | … |
| −0.2 | 3.747 | 3.717 |
| −0.3 | 3.865 | … |
| −0.4 | 3.954 | 3.892 |
| −0.5 | 3.940 | … |
| −0.6 | 3.540 | 4.048 |

| α | Present |
|---|---|
| 0.0 | 3.516 |
| 0.1 | 3.413 |
| 0.2 | 3.321 |
| 0.3 | 3.237 |
| 0.4 | 3.162 |
| 0.5 | 3.096 |
| 0.6 | 3.036 |

computed results with available results, we get percentage errors of 1.5% and 12.5% corresponding to taper parameter, α, of −0.4 and −0.6, respectively. Additionally, we have found that for *alpha* = −0.5, percentage error in computing pull-in voltage from the proposed method is less than 1% or 2% when compared with finite element method or semianalytical solution as mentioned by Joglekar and Pawaskar[40] in Table IV. Therefore, the approximation considered in non-uniform beam with linear taper in width gives negligible error when $|\alpha| \leq 0.4$, the percentage error for $0.5 \leq |\alpha| \leq 0.6$ can be assumed to be less than 12.5%. Thus, the approach adopted in this paper is validated and can be extended to compute frequencies of non-uniform beams with different tapering. Figure 2 shows variation of linear frequency with α for both converging and diverging beams with linear and quartic taper in width. We observe that the frequency for diverging beams decreases with an increase in α, while that of a converging beam increases. For converging

TABLE II. The non dimensional frequency of converging (negative α) and diverging (positive α) beam with quartic tapering in width.

| α | Frequency |
|---|---|
| 0.0 | 3.516 |
| −0.1 | 3.994 |
| −0.2 | 4.588 |
| −0.3 | 5.336 |
| −0.4 | 6.298 |
| −0.5 | 7.558 |
| −0.6 | 9.235 |

| α | Frequency |
|---|---|
| 0.0 | 3.516 |
| 0.1 | 3.124 |
| 0.2 | 2.799 |
| 0.3 | 2.526 |
| 0.4 | 2.294 |
| 0.5 | 2.096 |
| 0.6 | 1.924 |

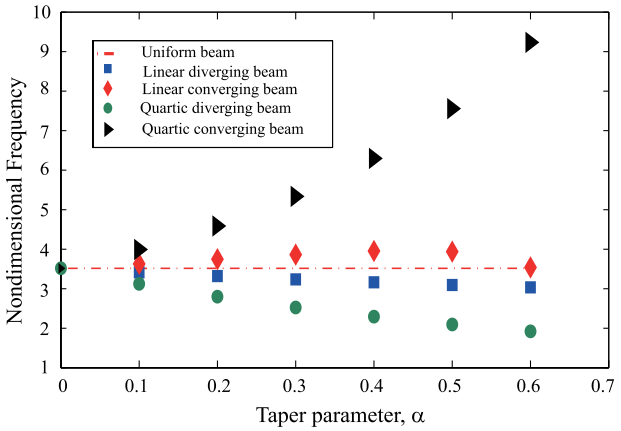


FIG. 2. Effect of taper parameter (α) on the linear frequency for various cases of tapering.

beam with quartic taper in width, the frequency is about 2.5 times greater than that of a uniform beam. The corresponding mode shape can be obtained for different beams for given values of α as discussed in Section II B. As a result, application of non-uniform cantilever beam (in particular, beams with quartic variation in width) can prove to be an excellent means in improving the performance of resonant sensors and actuators which operate at resonance frequency. In Secs. IV B and IV C, we discuss the pull-in voltage and the resonance frequency of various non-uniform beams by including the non-linear curvature effect.

### B. Pull-in analysis

To obtain the pull-in voltage for different tapered beams by following the approach as explained in Section III A, we first validate our model for pull-in voltage of a uniform beam with five different results from the literature as mentioned in Table III. Taking dimensions and material properties for each case as: (1) $L = 20\,000\,\mu$m, $b = 5000\,\mu$m, $h = 57\,\mu$m, $d_0 = 92\,\mu$m, $E' = 155.8$ GPa, and $v = 0.06$; (2) $L = 20\,000\,\mu$m, $b = 5000\,\mu$m, $h = 57\,\mu$m, $d_0 = 92\,\mu$m, $E' = 155.8$ GPa, and $v = 0.06$; (3) $L = 100\,\mu$m, $b = 50\,\mu$m, $h = 3\,\mu$m, $d_0 = 1\,\mu$m, $E' = 169$ GPa, and $v = 0.06$; (4) and (5) $L = 300\,\mu$m, $b = 50\,\mu$m, $h = 1\,\mu$m, $d_0 = 2.5\,\mu$m, $E' = 77$ GPa, and $v = 0.33$, computed results from the developed model are found to be in good agreement with available results. To compare the accuracy of non-uniform beam, when α is non-zero, we take few cases of converging beam with linear variation in width and compare the results with that of Joglekar and Pawaskar[40] in Table IV. The dimensions and the material

TABLE III. Comparison of the pull-in voltage of uniform cantilever beam with existing literature.

| Sample number | $V_{\text{Pull-in}}$ (V) (present model) | $V_{\text{Pull-in}}$ (V) (reference) | Reported by (method) |
|---|---|---|---|
| 1 | 65.19 | 68.5 | Hu *et al.*[44] (experimental) |
| 2 | 65.19 | 66.78 | Chaterjee and Pohit[29] (numerical) |
| 3 | 37.15 | 37.84 | Chowdhury *et al.*[26] (numerical) |
| 4 | 2.23 | 2.27 | Chowdhury *et al.*[26] (numerical) |
| 5 | 2.23 | 2.29 | Joglekar and Pawaskar[40] (analytical) |

TABLE IV. Comparison of the pull-in voltage of converging beam with linearly tapered width with existing literature.

| Sample number | $\alpha$ | Pull-in voltage by present model (V) | Pull-in voltage by Joglekar and Pawaskar[40] (V) |
|---|---|---|---|
| 1 | −0.25 | 5.45 | 5.59 (analytical) |
| 2 | −0.25 | 5.45 | 5.61 (FEA) |
| 3 | −0.5 | 24.74 | 24.26 (analytical) |
| 4 | −0.5 | 24.74 | 24.68 (FEA) |

properties for cases (1) and (2) are taken as $L = 200\,\mu$m, $b = 40\,\mu$m, $h = 1\,\mu$m, $d_0 = 2\,\mu$m, $E' = 169$ GPa, and $v = 0.06$, and that of (3) and (4) are taken as $L = 100\,\mu$m, $b = 15\,\mu$m, $h = 1\mu$m, $d_0 = 2\,\mu$m, $E' = 169$ GPa, and $v = 0.06$.

On comparing the pull-in voltage of linearly tapered beam for $\alpha = -0.25$ and $-0.5$ obtained from the present method with the results from Joglekar and Pawaskar[40] in Table IV, we get percentage error of about 2%. Although nonlinear curvature effect is neglected in their models, it may be insignificant for the given geometry. Now, we extend the analysis to different types of tapered beams. Figure 3(a) shows the pull-in voltage with different taper parameters ($\alpha$) for beams with linear and quartic variation in width. The dimensions and the material properties for each case are taken as $L = 200\,\mu$m, $b = 40\,\mu$m, $h = 1\,\mu$m, $d_0 = 2\,\mu$m, $E' = 168.39$ GPa, and $v = 0.06$. Figure 3(b) shows comparison of percentage difference in computing the pull-in voltage with and without fringing field effects of different non-uniform beams at different taper parameters. For a quartic tapered beam with taper parameter of $\alpha = -0.6$, we get a maximum percentage difference of about 7%. From our analysis, we find that for a converging beam, the pull-in voltage increases with an increase in $\alpha$, while for diverging beam, it decreases. This trend was expected because of the changes in stiffness of converging and diverging beam with $\alpha$. Similar changes were also observed in case of linear frequency in Sec. IV A. The linear frequency for diverging beam decreases with an increase in $\alpha$ which implies that stiffness effect (or spring force) decreases. As a result, at a lower voltage, the electrostatic forces balance the spring force, and then the pull-in occurs. While in case of converging beam, frequency (or stiffness) is more, and as a result a higher voltage is needed for electrostatic forces to overcome the spring force offered by cantilever beam. Consequently, we see that pull-in voltage increases by more than 100% in case of converging beam with quartic tapering as compared to uniform beam. Thus, employing a cantilever beam with quartic variation in width gives us a larger voltage threshold which is about 2 times as that of a widely used uniform beam for the operation of MEMS devices.

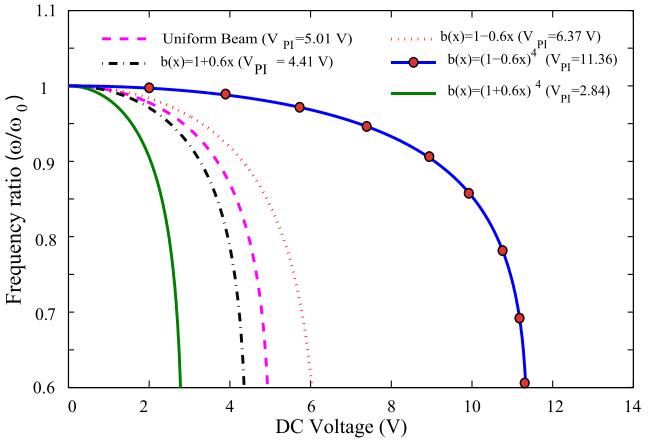


FIG. 4. Variation of linear, non-dimensional frequency with applied DC voltage for various types of beams. $\omega_0$ is the frequency at zero DC.

### C. Frequency analysis at finite DC

To study the vibration of different types of cantilever beams under the application of DC voltage, we solve the static deflection Eq. (23) at different $V$ to get static deflection $A$. Using obtained value of $A$, we find frequency from Eq. (28) for different values of DC voltage. Figure 4 shows variation of the frequency with applied DC for various types of beams. Frequencies are normalized with their corresponding frequencies at zero DC voltage. From Figure 4, we see that increase of DC voltage causes the system to soften and frequency decreases with an increase in voltage. We know that geometrical non-linearity has stiffening effect, while inertial nonlinearity and linear electrostatic forces have softening effect. However, overall effect on the dynamics depends on relative strength of each nonlinearity. In our analysis, we have neglected higher order terms of dynamic deflection in order to obtain the linear frequency at finite DC. With an increase of applied DC voltage, the linear frequency is found to decrease; thus, the system undergoes softening effect due to linear electrostatic forces. This trend is obtained as the

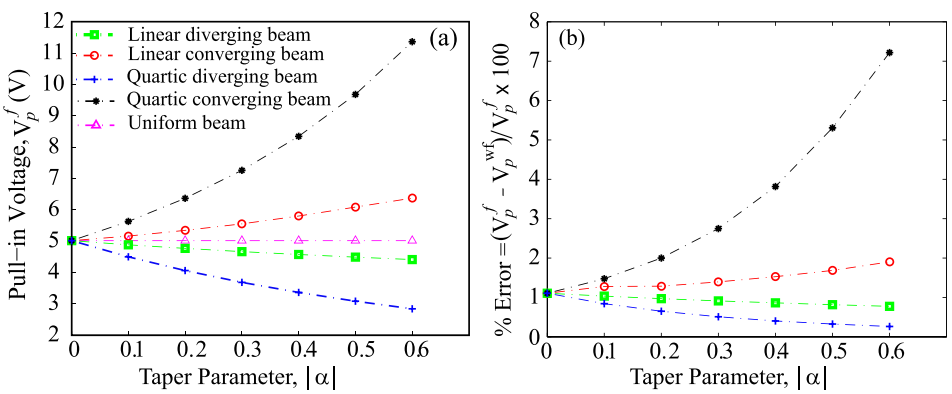


FIG. 3. (a) Effect of taper parameter ($\alpha$) on pull-in voltage $V_p^f$ including fringing effects for various cases of tapering. (b) Variation of percentage error in computing pull-in voltage with fringing effect, $V_p^f$, and without fringing effect, $V_p^{wf}$, with taper parameter.

initial gap to beam length ratio ($\gamma$) is less than 0.3 where the stiffening effect of geometrical nonlinearity is minimal. For $\gamma > 0.3$ and higher DC, the combined effect of geometrical nonlinearity and nonlinear electrostatic force with higher order terms becomes inevitable.[31] While this study considers geometrical nonlinearity, the higher order nonlinear terms of electrostatic forces are neglected.

## V. CONCLUSIONS

In this paper, we have developed theoretical model for computing the frequency as well as the pull-in voltage of non-uniform cantilever beam with nonlinear curvature effects. The non-uniformity considered in this paper is for the cantilever beams with linear and quartic tapering in width. To develop this model, we first obtained the exact mode shape from linear equation for beams with different non-uniformities. Subsequently, we apply the Galerkin method based on single mode shape to find the formulation for pull-in voltage and frequency from corresponding static and dynamic equations, respectively. From our analysis, we have observed that the linear frequency can be increased by more than 2.5 times, whereas the pull-in voltage can also be increased by 2 times simply by varying the order of tapering in the quartic tapered beam. Such findings can be utilized not just to increase the sensitivity of cantilever based devices, but it also increases the operating range of bias voltage.

## ACKNOWLEDGMENTS

We wish to acknowledge late Dr. A. P. J. Abdul Kalam for motivating us to do good science.

[1]K. L. Ekinci, X. M. H. Huang, and M. L. Roukes, Appl. Phys. Lett. **84**, 4469–4471 (2004).
[2]A. K. Pandey, O. Gottlieb, O. Shtempluck, and E. Buks, Appl. Phys. Lett. **96**, 203105 (2010).
[3]A. K. Pandey and R. Pratap, J. Micromech. Microeng. **17**(12), 2475 (2007).
[4]S. D. Vishwakarma, A. K. Pandey, J. M. Parpia, D. R. Southworth, H. G. Craighead, and R. Pratap, J. Microelectromech. Syst. **23**(2), 334–336 (2014).
[5]A. K. Pandey, J. Micromech. Microeng. **23**, 085015 (2013).
[6]P. N. Kambali, G. Swain, A. K. Pandey, E. Buks, and O. Gottlieb, Appl. Phys. Lett. **107**, 063104 (2015).
[7]A. K. Pandey, K. P. Venkatesh, and R. Pratap, Sadhana **34**(4), 651–662 (2009).
[8]I. Kozinsky, H. W. Ch. Postma, I. Bargatin, and M. L. Roukes, Appl. Phys. Lett. **88**, 253101 (2006).
[9]P. N. Kambali and A. K. Pandey, J. Comput. Nonlinear Dyn. **10**(5), 051010 (2015).
[10]H. C. Nathanson, W. E. Newell, R. Wickstrom, and J. R. Davis, Jr., IEEE Trans. Electron Devices **14**(3), 117–133 (1967).
[11]S. Pamidighantam, R. Puers, K. Baert, and H. A. Tilmans, J. Micromech. Microeng. **12**(4), 458 (2002).
[12]P. M. Osterberg and S. D. Senturia, J. Microelectromech. Syst. **6**(2), 107–118 (1997).
[13]H. A. Tilmans and R. Legtenberg, Sens. Actuators, A **45**(1), 67–84 (1994).
[14]Y. Fang and P. Li, J. Micromech. Microeng. **23**(4), 045010 (2013).
[15]A. H. Nayfeh, M. I. Younis, and E. M. Abdel-Rahman, Nonlinear Dyn. **41**(1–3), 211–236 (2005).
[16]A. H. Nayfeh, M. I. Younis, and E. M. Abdel-Rahman, Nonlinear Dyn. **48**(1–2), 153–163 (2007).
[17]R. D. Blevins and R. Plunkett, J. Appl. Mech. **47**, 461 (1980).
[18]H. H. Mabie and C. B. Rogers, J. Acoust. Soc. Am. **55**(5), 986–991 (1974).
[19]J. H. Lau, J. Appl. Mech. **51**(1), 179–181 (1984).
[20]H. H. Mabie and C. B. Rogers, J. Acoust. Soc. Am. **36**(3), 463–469 (1964).
[21]F. W. Williams and J. R. Banerjee, J. Sound Vib. **99**(1), 121–138 (1985).
[22]N. M. Auciello and G. Nole, J. Sound Vib. **214**(1), 105–119 (1998).
[23]H. C. Wang, J. Appl. Mech. **34**(3), 702–708 (1967).
[24]C. Y. Wang, Arch. Appl. Mech. **83**(1), 171–176 (2013).
[25]S. Abrate, J. Sound Vib. **185**(4), 703–716 (1995).
[26]S. Chowdhury, M. Ahmadi, and W. C. Miller, J. Micromech. Microeng. **15**(4), 756 (2005).
[27]N. P. Van Der Meijs and J. T. Fokkema, Integration, VLSI J. **2**(2), 85–119 (1984).
[28]K. Ramakrishnan and H. Srinivasan, J. Electr. Eng. **63**(4), 242–248 (2012).
[29]S. Chaterjee and G. Pohit, J. Sound Vib. **322**(4), 969–986 (2009).
[30]G. Li and N. R. Aluru, Sens. Actuators, A **91**(3), 278–291 (2001).
[31]M. Rasekh and S. E. Khadem, Int. J. Mech. Sci. **53**(2), 108–115 (2011).
[32]M. Rahaeifard, M. H. Kahrobaiyan, M. Asghari, and M. T. Ahmadian, Sens. Actuators, A **171**(2), 370–374 (2011).
[33]M. Baghani, Int. J. Eng. Sci. **54**, 99–105 (2012).
[34]J. Cheng, J. Zhe, and X. Wu, J. Micromech. Microeng. **14**(1), 57 (2004).
[35]E. Lemaire, V. Rochus, J. C. Golinval, and P. Duysinx, Comput. Methods Appl. Mech. Eng. **197**(45), 4040–4050 (2008).
[36]M. Raulli and K. Maute, Struct. Multidiscip. Optim. **30**(5), 342–359 (2005).
[37]M. M. Abdalla, C. K. Reddy, W. F. Faris, and Z. Grdal, Comput. Struct. **83**(15), 1320–1329 (2005).
[38]F. Najar, S. Choura, E. M. Abdel-Rahman, S. El-Borgi, and A. Nayfeh, J. Micromech. Microeng. **16**(11), 2449 (2006).
[39]F. Najar, S. Choura, S. El-Borgi, E. M. Abdel-Rahman, and A. H. Nayfeh, J. Micromech. Microeng. **15**(3), 419 (2005).
[40]M. M. Joglekar and D. N. Pawaskar, Microsyst. Technol. **17**(1), 35–45 (2011).
[41]H. Shang-Rou, S. W. Shaw, and C. Pierre, Int. J. Solids Struct. **31**(14), 1981–2014 (1994).
[42]D. H. Hodges, AIAA J. **22**(12), 1825–1827 (1984).
[43]L. Meirovitch, *Elements of Vibration Analysis* (McGraw-Hill, New York, 1986), Vol. 2.
[44]Y. C. Hu, C. M. Chang, and S. C. Huang, Sens. Actuators, A **112**(1), 155–161 (2004).